Percellome Explorer ver. 0.5.0 : PDBEx_RSort_Expand_H_G2_AP_Std-Av@
Target Prj: vs TTG194-L // TTG4: A) Valproic acid sodium salt, B) Valproic acid sodium salt (TTG4(2+1))
Denominator: Target * Candidate

Name	Condition	Num	Cor
TTG194-L	TTG4: A) Valproic acid sodium salt, B) Valproic acid sodium salt (TTG4(2+1))	5057	1.977
TTG151-L	Valproic acid sodium salt x Valproic acid sodium salt	1432	0.782
TTG193-L	TTG4: A) Valproic acid sodium salt, B) Valproic acid sodium salt (TTG4(1+1))	1291	0.754
TTG195-L	TTG4: A) Valproic acid sodium salt, B) Valproic acid sodium salt (TTG4(4+1))	1619	0.754
TTG157-L	Valproic acid sodium salt	1591	0.664
TTG202-L	TTG4: A) Clofibrate, B) Clofibrate (TTG4(4+1))	493	0.504
TTG041-L	Valproic acid sodium salt	1424	0.493
TTG200-L	TTG4: A) Clofibrate, B) Clofibrate (TTG4(1+1))	481	0.469
TTG044-L	Clofibrate	741	0.442
TTG201-L	TTG4: A) Clofibrate, B) Clofibrate (TTG4(2+1))	469	0.431
TTG098-L	DEHP	1232	0.429
TTG199-L	Black No.401	342	0.427
TTG118-L	Clofibrate x Clofibrate	744	0.417
TTG141-L	Tributyltin chloride x Clofibrate	876	0.394
TTG129-L	CCl4 x Clofibrate	578	0.389
TTG206-L	BTAZ3864(CoCAM 2)	1811	0.384
TTG019-L	2-Vinylpyridine	395	0.378
TTG149-L	Valproic acid sodium salt x Aspirin	513	0.367
TTG168-L	Mastic	491	0.367
TTG016-L	Pentachlorophenol	552	0.365
TTG137-L	alpha-Lipoic Acid	348	0.36
TTG162-L	Sesame seed oil unsaponified matter	569	0.358
TTG188-L	Violet No.401	258	0.358
TTG062-L(C)	Dexamethasone	553	0.355
TTG104-L	MEHP	972	0.353
TTG189-L	TTG4: A) CCl4, B) Ccl4 (TTG4(1+1))	469	0.353
TTG032-L	3-Amino-1H-1,2,4-triazole	1180	0.352
TTG051-L	9-cis retinoic acid	283	0.352
TTG060-L	Forskolin	240	0.351
TTG047-L	Bisphenol A (PLD)	279	0.35
TTG120-L	Clofibrate x PCN	501	0.348
TTG184-L	Bisphenol A/ERaKO(Chambon) (corn oil)	313	0.348
TTG059-L	Caffeine	404	0.346
TTG147-L	Estragole	327	0.346
TTG066-L	Methoprene	328	0.343
TTG183-L	Bisphenol A (corn oil)	358	0.343
TTG154-L	Sodium Dehydroacetate	684	0.342
TTG029-L	2-Aminomethylpyridine	136	0.34
TTG140-L	Food Red No.40	318	0.338
TTG182-L	Imidacloprid	573	0.337
TTG165-L	Chlorpyrifos	341	0.336
TTG088-L	Tebufenozide	168	0.334
TTG042-L	Ethynyl estradiol (PLD)	276	0.332
TTG097-L	Permethrin	178	0.332
TTG073-L	Toluene	499	0.331
TTG205-L	BTAZ3846(CoCAM 1)	2021	0.326
TTG155-L	Aluminum ammonium sulfate	362	0.323
TTG070-L	Formaldehyde	124	0.321
TTG161-L	Food Yellow No.4	443	0.321
TTG136-L	Phytol	765	0.32
TTG177-L	Red No.102	282	0.319
TTG139-L	Indigo Carmine	388	0.314
TTG016-L(C)	Pentachlorophenol	700	0.313
TTG057-L	Indigo	168	0.311
TTG144-L	Tributyltin chloride x Phenobarbital	456	0.311
TTG091-L	Azacytidine	265	0.31
TTG115-L	Kanamycin monosulfate	209	0.31
TTG094-L	Aspirin	453	0.307
TTG043-L	Testosterone propionate	253	0.305
TTG077-L	Monocrotaline	189	0.304
TTG093-L	AraC	332	0.304
TTG090-L	Pregnenolone Carbonitrile	453	0.303
TTG126-L	Thalidomide	276	0.302

Percellome Explorer ver. 0.5.0 : PDBEx_RSort_Expand_H_G2_AP_Std-Av@
Target Prj: vs TTG195-L // TTG4: A) Valproic acid sodium salt, B) Valproic acid sodium salt (TTG4(4+1))
Denominator: Target * Candidate

Name	Condition	Num	Cor
TTG195-L	TTG4: A) Valproic acid sodium salt, B) Valproic acid sodium salt (TTG4(4+1))	4246	2.355
TTG193-L	TTG4: A) Valproic acid sodium salt, B) Valproic acid sodium salt (TTG4(1+1))	1299	0.903
TTG151-L	Valproic acid sodium salt x Valproic acid sodium salt	1279	0.832
TTG157-L	Valproic acid sodium salt	1590	0.79
TTG194-L	TTG4: A) Valproic acid sodium salt, B) Valproic acid sodium salt (TTG4(2+1))	1619	0.754
TTG118-L	Clofibrate x Clofibrate	873	0.583
TTG200-L	TTG4: A) Clofibrate, B) Clofibrate (TTG4(1+1))	500	0.581
TTG044-L	Clofibrate	795	0.564
TTG202-L	TTG4: A) Clofibrate, B) Clofibrate (TTG4(4+1))	463	0.563
TTG041-L	Valproic acid sodium salt	1320	0.545
TTG129-L	CCl4 x Clofibrate	647	0.519
TTG098-L	DEHP	1247	0.517
TTG141-L	Tributyltin chloride x Clofibrate	907	0.486
TTG199-L	Black No.401	325	0.484
TTG201-L	TTG4: A) Clofibrate, B) Clofibrate (TTG4(2+1))	427	0.467
TTG206-L	BTAZ3864(CoCAM 2)	1764	0.446
TTG019-L	2-Vinylpyridine	390	0.445
TTG120-L	Clofibrate x PCN	532	0.44
TTG154-L	Sodium Dehydroacetate	735	0.438
TTG165-L	Chlorpyrifos	368	0.432
TTG094-L	Aspirin	532	0.429
TTG066-L	Methoprene	342	0.425
TTG062-L(C)	Dexamethasone	554	0.424
TTG016-L(C)	Pentachlorophenol	793	0.423
TTG189-L	TTG4: A) CCl4, B) Ccl4 (TTG4(1+1))	472	0.423
TTG059-L	Caffeine	413	0.422
TTG182-L	Imidacloprid	602	0.422
TTG149-L	Valproic acid sodium salt x Aspirin	492	0.419
TTG032-L	3-Amino-1H-1,2,4-triazole	1165	0.414
TTG016-L	Pentachlorophenol	521	0.411
TTG136-L	Phytol	826	0.411
TTG104-L	MEHP	943	0.408
TTG047-L	Bisphenol A (PLD)	270	0.404
TTG070-L	Formaldehyde	129	0.398
TTG168-L	Mastic	445	0.397
TTG060-L	Forskolin	226	0.394
TTG205-L	BTAZ3846(CoCAM 1)	2034	0.391
TTG188-L	Violet No.401	236	0.39
TTG144-L	Tributyltin chloride x Phenobarbital	477	0.387
TTG097-L	Permethrin	174	0.386
TTG087-L	Pyriproxyfen	361	0.385
TTG162-L	Sesame seed oil unsaponified matter	510	0.382
TTG077-L	Monocrotaline	197	0.377
TTG088-L	Tebufenozide	159	0.377
TTG155-L	Aluminum ammonium sulfate	355	0.377
TTG147-L	Estragole	298	0.376
TTG073-L	Toluene	474	0.374
TTG074-L	Bromobenzene	727	0.372
TTG184-L	Bisphenol A/ERaKO(Chambon) (corn oil)	280	0.37
TTG183-L	Bisphenol A (corn oil)	323	0.368
TTG061-L	Paraquat dichloride	403	0.366
TTG177-L	Red No.102	272	0.366
TTG078-L	Ethanol	228	0.362
TTG029-L	2-Aminomethylpyridine	121	0.361
TTG089-L	Rifampicin	254	0.361
TTG091-L	Azacytidine	259	0.36
TTG126-L	Thalidomide	276	0.36
TTG137-L	alpha-Lipoic Acid	292	0.36
TTG093-L	AraC	330	0.359
TTG058-L	Diethylnitrosamine (C3H)	208	0.358
TTG079-L	Methanol	299	0.358
TTG037-L	Phenobarbital	843	0.356
TTG031-L	2-Chloro-4,6-dimethylaniline	435	0.355

Percellome Explorer ver. 0.5.0 : PDBEx_RSort_Expand_H_G2_AP_Std-Av@
Target Prj: vs TTG199-L // Black No.401
Denominator: Target * Candidate

Name	Condition	Num	Cor
TTG199-L	Black No.401	1582	6.321
TTG200-L	TTG4: A) Clofibrate, B) Clofibrate (TTG4(1+1))	174	0.542
TTG188-L	Violet No.401	118	0.523
TTG019-L	2-Vinylpyridine	165	0.505
TTG195-L	TTG4: A) Valproic acid sodium salt, B) Valproic acid sodium salt (TTG4(4+1))	325	0.484
TTG060-L	Forskolin	98	0.459
TTG066-L	Methoprene	137	0.457
TTG120-L	Clofibrate x PCN	204	0.453
TTG044-L	Clofibrate	237	0.452
TTG033-L	1,2-Dichloro-3-nitrobenzene	111	0.449
TTG121-L	Clofibrate x ATRA	157	0.446
TTG162-L	Sesame seed oil unsaponified matter	219	0.44
TTG193-L	TTG4: A) Valproic acid sodium salt, B) Valproic acid sodium salt (TTG4(1+1))	236	0.44
TTG144-L	Tributyltin chloride x Phenobarbital	200	0.436
TTG189-L	TTG4: A) CCl4, B) Ccl4 (TTG4(1+1))	181	0.435
TTG098-L	DEHP	388	0.432
TTG183-L	Bisphenol A (corn oil)	141	0.432
TTG194-L	TTG4: A) Valproic acid sodium salt, B) Valproic acid sodium salt (TTG4(2+1))	342	0.427
TTG123-L	Caffeine	118	0.424
TTG016-L	Pentachlorophenol	200	0.423
TTG051-L	9-cis retinoic acid	106	0.421
TTG140-L	Food Red No.40	124	0.421
TTG151-L	Valproic acid sodium salt x Valproic acid sodium salt	238	0.415
TTG184-L	Bisphenol A/ERaKO(Chambon) (corn oil)	117	0.415
TTG177-L	Red No.102	113	0.408
TTG134-L	Nerolidol	79	0.405
TTG073-L	Toluene	190	0.403
TTG149-L	Valproic acid sodium salt x Aspirin	176	0.402
TTG202-L	TTG4: A) Clofibrate, B) Clofibrate (TTG4(4+1))	123	0.402
TTG043-L	Testosterone propionate	104	0.401
TTG077-L	Monocrotaline	78	0.401
TTG094-L	Aspirin	185	0.4
TTG137-L	alpha-Lipoic Acid	119	0.394
TTG090-L	Pregnenolone Carbonitrile	184	0.393
TTG042-L	Ethynyl estradiol (PLD)	102	0.392
TTG141-L	Tributyltin chloride x Clofibrate	271	0.39
TTG168-L	Mastic	163	0.39
TTG187-L	Violet No.201	129	0.39
TTG088-L	Tebufenozide	61	0.388
TTG165-L	Chlorpyrifos	123	0.387
TTG206-L	BTAZ3864(CoCAM 2)	567	0.385
TTG032-L	3-Amino-1H-1,2,4-triazole	399	0.381
TTG157-L	Valproic acid sodium salt	286	0.381
TTG139-L	Indigo Carmine	147	0.38
TTG136-L	Phytol	281	0.376
TTG097-L	Permethrin	63	0.375
TTG129-L	CCl4 x Clofibrate	174	0.375
TTG031-L	2-Chloro-4,6-dimethylaniline	170	0.373
TTG126-L	Thalidomide	106	0.371
TTG028-L	1,2,4-Triazole	99	0.37
TTG059-L	Caffeine	135	0.37
TTG118-L	Clofibrate x Clofibrate	206	0.369
TTG117-L	Digitoxin	117	0.367
TTG182-L	Imidacloprid	195	0.367
TTG154-L	Sodium Dehydroacetate	229	0.366
TTG058-L	Diethylnitrosamine (C3H)	79	0.365
TTG055-L	N-ethy1-N-nitrosourea	78	0.363
TTG104-L	MEHP	311	0.361
TTG176-L	Green No.204 (Pyranine Conc)	83	0.361
TTG016-L(C)	Pentachlorophenol	252	0.36
TTG079-L	Methanol	112	0.36
TTG147-L	Estragole	106	0.359
TTG074-L	Bromobenzene	261	0.358

Percellome Explorer ver. 0.5.0 : PDBEx_RSort_Expand_H_G2_AP_Std-Av@
Target Prj: vs TTG200-L // TTG4: A) Clofibrate, B) Clofibrate (TTG4(1+1))
Denominator: Target * Candidate

Name	Condition	Num	Cor
TTG200-L	TTG4: A) Clofibrate, B) Clofibrate (TTG4(1+1))	2028	4.931
TTG202-L	TTG4: A) Clofibrate, B) Clofibrate (TTG4(4+1))	399	1.016
TTG201-L	TTG4: A) Clofibrate, B) Clofibrate (TTG4(2+1))	393	0.9
TTG129-L	CCl4 x Clofibrate	507	0.852
TTG044-L	Clofibrate	572	0.85
TTG118-L	Clofibrate x Clofibrate	570	0.797
TTG141-L	Tributyltin chloride x Clofibrate	649	0.729
TTG098-L	DEHP	767	0.666
TTG104-L	MEHP	677	0.613
TTG195-L	TTG4: A) Valproic acid sodium salt, B) Valproic acid sodium salt (TTG4(4+1))	500	0.581
TTG193-L	TTG4: A) Valproic acid sodium salt, B) Valproic acid sodium salt (TTG4(1+1))	392	0.571
TTG147-L	Estragole	208	0.549
TTG199-L	Black No.401	174	0.542
TTG016-L	Pentachlorophenol	325	0.536
TTG151-L	Valproic acid sodium salt x Valproic acid sodium salt	381	0.519
TTG095-L	Ibuprofen (dl-p-isobutylhydratropic acid)	217	0.512
TTG206-L	BTAZ3864(CoCAM 2)	950	0.503
TTG070-L	Formaldehyde	76	0.491
TTG073-L	Toluene	295	0.488
TTG019-L	2-Vinylpyridine	200	0.478
TTG051-L	9-cis retinoic acid	153	0.474
TTG168-L	Mastic	254	0.474
TTG087-L	Pyriproxyfen	212	0.473
TTG134-L	Nerolidol	118	0.472
TTG194-L	TTG4: A) Valproic acid sodium salt, B) Valproic acid sodium salt (TTG4(2+1))	481	0.469
TTG133-L	Maltol	131	0.464
TTG120-L	Clofibrate x PCN	264	0.457
TTG189-L	TTG4: A) CCl4, B) Ccl4 (TTG4(1+1))	243	0.456
TTG115-L	Kanamycin monosulfate	123	0.455
TTG062-L(C)	Dexamethasone	279	0.447
TTG059-L	Caffeine	208	0.445
TTG066-L	Methoprene	167	0.435
TTG154-L	Sodium Dehydroacetate	342	0.427
TTG162-L	Sesame seed oil unsaponified matter	271	0.425
TTG029-L	2-Aminomethylpyridine	68	0.424
TTG088-L	Tebufenozide	85	0.422
TTG205-L	BTAZ3846(CoCAM 1)	1044	0.42
TTG139-L	Indigo Carmine	207	0.418
TTG165-L	Chlorpyrifos	170	0.418
TTG135-L	Methyl dihydro jasmonate	107	0.414
TTG136-L	Phytol	396	0.413
TTG182-L	Imidacloprid	281	0.413
TTG060-L	Forskolin	112	0.409
TTG188-L	Violet No.401	118	0.408
TTG094-L	Aspirin	241	0.407
TTG121-L	Clofibrate x ATRA	184	0.407
TTG157-L	Valproic acid sodium salt	390	0.406
TTG137-L	alpha-Lipoic Acid	156	0.403
TTG041-L	Valproic acid sodium salt	459	0.397
TTG191-L	TTG4: A) CCl4, B) Ccl4 (TTG4(4+1))	116	0.394
TTG149-L	Valproic acid sodium salt x Aspirin	220	0.392
TTG043-L	Testosterone propionate	130	0.391
TTG124-L	Vat Red I	146	0.389
TTG026-L	TCDF(2,3,7,8-Tetrachlorodibenzofuran)	218	0.385
TTG016-L(C)	Pentachlorophenol	344	0.384
TTG144-L	Tributyltin chloride x Phenobarbital	226	0.384
TTG109-L	Acephate	263	0.383
TTG031-L	2-Chloro-4,6-dimethylaniline	221	0.378
TTG047-L	Bisphenol A (PLD)	120	0.376
TTG126-L	Thalidomide	137	0.374
TTG184-L	Bisphenol A/ERaKO(Chambon) (corn oil)	134	0.371
TTG177-L	Red No.102	131	0.369
TTG057-L	Indigo	79	0.365

Percellome Explorer ver. 0.5.0 : PDBEx_RSort_Expand_H_G2_AP_Std-Av@
Target Prj: vs TTG201-L // TTG4: A) Clofibrate, B) Clofibrate (TTG4(2+1))
Denominator: Target * Candidate

Name	Condition	Num	Cor
TTG201-L	TTG4: A) Clofibrate, B) Clofibrate (TTG4(2+1))	2152	4.647
TTG202-L	TTG4: A) Clofibrate, B) Clofibrate (TTG4(4+1))	409	0.982
TTG200-L	TTG4: A) Clofibrate, B) Clofibrate (TTG4(1+1))	393	0.9
TTG129-L	CCl4 x Clofibrate	443	0.701
TTG044-L	Clofibrate	500	0.7
TTG118-L	Clofibrate x Clofibrate	492	0.648
TTG141-L	Tributyltin chloride x Clofibrate	530	0.561
TTG095-L	Ibuprofen (dl-p-isobutylhydratropic acid)	240	0.534
TTG098-L	DEHP	627	0.513
TTG104-L	MEHP	575	0.491
TTG195-L	TTG4: A) Valproic acid sodium salt, B) Valproic acid sodium salt (TTG4(4+1))	427	0.467
TTG147-L	Estragole	187	0.465
TTG051-L	9-cis retinoic acid	154	0.45
TTG151-L	Valproic acid sodium salt x Valproic acid sodium salt	341	0.437
TTG193-L	TTG4: A) Valproic acid sodium salt, B) Valproic acid sodium salt (TTG4(1+1))	317	0.435
TTG194-L	TTG4: A) Valproic acid sodium salt, B) Valproic acid sodium salt (TTG4(2+1))	469	0.431
TTG121-L	Clofibrate x ATRA	196	0.409
TTG135-L	Methyl dihydro jasmonate	110	0.401
TTG206-L	BTAZ3864(CoCAM 2)	796	0.397
TTG062-L(C)	Dexamethasone	259	0.391
TTG077-L	Monocrotaline	103	0.389
TTG059-L	Caffeine	188	0.379
TTG028-L	1,2,4-Triazole	133	0.365
TTG168-L	Mastic	205	0.361
TTG029-L	2-Aminomethylpyridine	61	0.359
TTG157-L	Valproic acid sodium salt	363	0.356
TTG188-L	Violet No.401	109	0.355
TTG060-L	Forskolin	102	0.351
TTG097-L	Permethrin	80	0.35
TTG134-L	Nerolidol	93	0.35
TTG199-L	Black No.401	119	0.35
TTG070-L	Formaldehyde	57	0.347
TTG055-L	N-ethy1-N-nitrosourea	101	0.345
TTG137-L	alpha-Lipoic Acid	142	0.345
TTG149-L	Valproic acid sodium salt x Aspirin	205	0.345
TTG178-L	Aluminum sulfate	164	0.342
TTG109-L	Acephate	248	0.341
TTG190-L	TTG4: A) CCl4, B) Ccl4 (TTG4(2+1))	90	0.341
TTG162-L	Sesame seed oil unsaponified matter	229	0.339
TTG041-L	Valproic acid sodium salt	407	0.331
TTG140-L	Food Red No.40	132	0.33
TTG120-L	Clofibrate x PCN	201	0.328
TTG073-L	Toluene	210	0.327
TTG177-L	Red No.102	122	0.324
TTG176-L	Green No.204 (Pyranine Conc)	101	0.323
TTG124-L	Vat Red I	128	0.322
TTG166-L	Carbaryl	201	0.322
TTG161-L	Food Yellow No.4	188	0.321
TTG133-L	Maltol	96	0.32
TTG144-L	Tributyltin chloride x Phenobarbital	198	0.317
TTG080-L	DMSO	90	0.316
TTG158-L	Deet x Permethrin	138	0.316
TTG148-L	Verbenone	90	0.315
TTG016-L	Pentachlorophenol	202	0.314
TTG094-L	Aspirin	196	0.312
TTG205-L	BTAZ3846(CoCAM 1)	818	0.31
TTG130-L	CCl4 x CCl4	80	0.308
TTG191-L	TTG4: A) CCl4, B) Ccl4 (TTG4(4+1))	96	0.307
TTG042-L	Ethynyl estradiol (PLD)	108	0.305
TTG123-L	Caffeine	115	0.303
TTG154-L	Sodium Dehydroacetate	258	0.303
TTG131B-L	CCl4 x Phenobarbital	187	0.302
TTG139-L	Indigo Carmine	159	0.302

Percellome Explorer ver. 0.5.0 : PDBEx_RSort_Expand_H_G2_AP_Std-Av@
Target Prj: vs TTG202-L // TTG4: A) Clofibrate, B) Clofibrate (TTG4(4+1))
Denominator: Target * Candidate

Name	Condition	Num	Cor
TTG202-L	TTG4: A) Clofibrate, B) Clofibrate (TTG4(4+1))	1936	5.165
TTG200-L	TTG4: A) Clofibrate, B) Clofibrate (TTG4(1+1))	399	1.016
TTG201-L	TTG4: A) Clofibrate, B) Clofibrate (TTG4(2+1))	409	0.982
TTG129-L	CCl4 x Clofibrate	471	0.829
TTG044-L	Clofibrate	497	0.774
TTG118-L	Clofibrate x Clofibrate	526	0.77
TTG141-L	Tributyltin chloride x Clofibrate	559	0.657
TTG095-L	Ibuprofen (dl-p-isobutylhydratropic acid)	259	0.641
TTG147-L	Estragole	205	0.567
TTG195-L	TTG4: A) Valproic acid sodium salt, B) Valproic acid sodium salt (TTG4(4+1))	463	0.563
TTG193-L	TTG4: A) Valproic acid sodium salt, B) Valproic acid sodium salt (TTG4(1+1))	368	0.561
TTG098-L	DEHP	611	0.556
TTG104-L	MEHP	559	0.53
TTG029-L	2-Aminomethylpyridine	78	0.51
TTG194-L	TTG4: A) Valproic acid sodium salt, B) Valproic acid sodium salt (TTG4(2+1))	493	0.504
TTG062-L(C)	Dexamethasone	298	0.5
TTG151-L	Valproic acid sodium salt x Valproic acid sodium salt	350	0.499
TTG051-L	9-cis retinoic acid	152	0.493
TTG206-L	BTAZ3864(CoCAM 2)	838	0.465
TTG188-L	Violet No.401	128	0.464
TTG178-L	Aluminum sulfate	198	0.458
TTG059-L	Caffeine	204	0.457
TTG157-L	Valproic acid sodium salt	408	0.445
TTG028-L	1,2,4-Triazole	145	0.443
TTG135-L	Methyl dihydro jasmonate	109	0.442
TTG133-L	Maltol	119	0.441
TTG088-L	Tebufenozide	83	0.431
TTG121-L	Clofibrate x ATRA	185	0.429
TTG187-L	Violet No.201	174	0.429
TTG077-L	Monocrotaline	102	0.428
TTG080-L	DMSO	109	0.425
TTG134-L	Nerolidol	100	0.419
TTG039-L	Citric acid-calcium salt	98	0.412
TTG079-L	Methanol	156	0.409
TTG097-L	Permethrin	84	0.409
TTG120-L	Clofibrate x PCN	225	0.408
TTG168-L	Mastic	207	0.405
TTG154-L	Sodium Dehydroacetate	309	0.404
TTG199-L	Black No.401	123	0.402
TTG060-L	Forskolin	104	0.398
TTG149-L	Valproic acid sodium salt x Aspirin	211	0.394
TTG165-L	Chlorpyrifos	153	0.394
TTG049-L	Tributyltin chloride	93	0.391
TTG167-L	Aloe arborescens extract	112	0.389
TTG055-L	N-ethy1-N-nitrosourea	100	0.38
TTG085-L	Trybutyltin	144	0.378
TTG094-L	Aspirin	214	0.378
TTG041-L	Valproic acid sodium salt	416	0.377
TTG183-L	Bisphenol A (corn oil)	149	0.373
TTG109-L	Acephate	242	0.369
TTG019-L	2-Vinylpyridine	147	0.368
TTG155-L	Aluminum ammonium sulfate	158	0.368
TTG073-L	Toluene	212	0.367
TTG166-L	Carbaryl	204	0.363
TTG148-L	Verbenone	93	0.362
TTG162-L	Sesame seed oil unsaponified matter	220	0.362
TTG031-L	2-Chloro-4,6-dimethylaniline	200	0.358
TTG047-L	Bisphenol A (PLD)	109	0.357
TTG137-L	alpha-Lipoic Acid	132	0.357
TTG170-L	3-methylcholanthrene/AhRKO	112	0.357
TTG205-L	BTAZ3846(CoCAM 1)	848	0.357
TTG027-L	1,2,3-Triazole	115	0.356
TTG034-L	4-Ethylnitrobenzene	100	0.355

Percellome Explorer ver. 0.5.0 : PDBEx_RSort_Expand_H_G2_AP_Std-Av@
Target Prj: vs TTG204-L // Red No.225
Denominator: Target * Candidate

Name	Condition	Num	Cor
TTG204-L	Red No.225	4199	2.382
TTG020-L	TCDD(2,3,7,8-Tetrachlorodibenzo-p-Dioxin)	754	0.601
TTG144-L	Tributyltin chloride x Phenobarbital	677	0.556
TTG120-L	Clofibrate x PCN	627	0.524
TTG162-L	Sesame seed oil unsaponified matter	661	0.501
TTG098-L	DEHP	1174	0.492
TTG016-L	Pentachlorophenol	581	0.463
TTG056-L	3-methylcholanthrene	585	0.463
TTG090-L	Pregnenolone Carbonitrile	575	0.463
TTG206-L	BTAZ3864(CoCAM 2)	1644	0.42
TTG104-L	MEHP	928	0.406
TTG168-L	Mastic	447	0.403
TTG016-L(C)	Pentachlorophenol	747	0.402
TTG037-L	Phenobarbital	929	0.396
TTG131B-L	CCl4 x Phenobarbital	475	0.393
TTG026-L	TCDF(2,3,7,8-Tetrachlorodibenzofuran)	460	0.392
TTG183-L	Bisphenol A (corn oil)	339	0.391
TTG187-L	Violet No.201	341	0.388
TTG019-L	2-Vinylpyridine	332	0.383
TTG057-L	Indigo	170	0.379
TTG070-L	Formaldehyde	120	0.374
TTG124-L	Vat Red I	287	0.37
TTG043-L	Testosterone propionate	254	0.369
TTG015-L	4-amino-2,6-dichlorophenol	151	0.367
TTG205-L	BTAZ3846(CoCAM 1)	1888	0.367
TTG141-L	Tributyltin chloride x Clofibrate	675	0.366
TTG033-L	1,2-Dichloro-3-nitrobenzene	239	0.365
TTG200-L	TTG4: A) Clofibrate, B) Clofibrate (TTG4(1+1))	308	0.362
TTG032-L	3-Amino-1H-1,2,4-triazole	1000	0.359
TTG151-L	Valproic acid sodium salt x Valproic acid sodium salt	538	0.354
TTG031-L	2-Chloro-4,6-dimethylaniline	428	0.353
TTG129-L	CCl4 x Clofibrate	435	0.353
TTG137-L	alpha-Lipoic Acid	283	0.353
TTG118-L	Clofibrate x Clofibrate	520	0.351
TTG028-L	1,2,4-Triazole	245	0.345
TTG066-L	Methoprene	273	0.343
TTG193-L	TTG4: A) Valproic acid sodium salt, B) Valproic acid sodium salt (TTG4(1+1))	486	0.342
TTG195-L	TTG4: A) Valproic acid sodium salt, B) Valproic acid sodium salt (TTG4(4+1))	602	0.338
TTG044-L	Clofibrate	469	0.337
TTG047-L	Bisphenol A (PLD)	223	0.337
TTG199-L	Black No.401	223	0.336
TTG132-L	Curcumin	536	0.333
TTG046-L	Levothyroxine	409	0.33
TTG184-L	Bisphenol A/ERaKO(Chambon) (corn oil)	243	0.325
TTG041-L	Valproic acid sodium salt	774	0.323
TTG091-L	Azacytidine	226	0.318
TTG126-L	Thalidomide	240	0.316
TTG149-L	Valproic acid sodium salt x Aspirin	366	0.315
TTG136-L	Phytol	621	0.313
TTG182-L	Imidacloprid	441	0.313
TTG109-L	Acephate	441	0.31
TTG155-L	Aluminum ammonium sulfate	288	0.31
TTG188-L	Violet No.401	185	0.309
TTG190-L	TTG4: A) CCl4, B) Ccl4 (TTG4(2+1))	159	0.308
TTG189-L	TTG4: A) CCl4, B) Ccl4 (TTG4(1+1))	340	0.308
TTG027-L	1,2,3-Triazole	214	0.305
TTG134-L	Nerolidol	158	0.305
TTG135-L	Methyl dihydro jasmonate	163	0.305
TTG086-L	Coenzyme Q10	479	0.304
TTG093-L	AraC	276	0.304
TTG073-L	Toluene	378	0.302
TTG147-L	Estragole	237	0.302
TTG029-L	2-Aminomethylpyridine	100	0.301

Percellome Explorer ver. 0.5.0 : PDBEx_RSort_Expand_H_G2_AP_Std-Av@
Target Prj: vs TTG205-L // BTAZ3846(CoCAM 1)
Denominator: Target * Candidate

Name	Condition	Num	Cor
TTG205-L	BTAZ3846(CoCAM 1)	12257	0.816
TTG206-L	BTAZ3864(CoCAM 2)	6508	0.57
TTG098-L	DEHP	3864	0.555
TTG118-L	Clofibrate x Clofibrate	2116	0.489
TTG044-L	Clofibrate	1960	0.482
TTG141-L	Tributyltin chloride x Clofibrate	2590	0.481
TTG129-L	CCl4 x Clofibrate	1691	0.47
TTG104-L	MEHP	3086	0.462
TTG016-L	Pentachlorophenol	1628	0.445
TTG120-L	Clofibrate x PCN	1519	0.435
TTG151-L	Valproic acid sodium salt x Valproic acid sodium salt	1864	0.42
TTG200-L	TTG4: A) Clofibrate, B) Clofibrate (TTG4(1+1))	1044	0.42
TTG144-L	Tributyltin chloride x Phenobarbital	1470	0.414
TTG193-L	TTG4: A) Valproic acid sodium salt, B) Valproic acid sodium salt (TTG4(1+1))	1641	0.395
TTG032-L	3-Amino-1H-1,2,4-triazole	3187	0.392
TTG195-L	TTG4: A) Valproic acid sodium salt, B) Valproic acid sodium salt (TTG4(4+1))	2034	0.391
TTG037-L	Phenobarbital	2645	0.387
TTG073-L	Toluene	1374	0.376
TTG019-L	2-Vinylpyridine	947	0.374
TTG041-L	Valproic acid sodium salt	2591	0.37
TTG204-L	Red No.225	1888	0.367
TTG136-L	Phytol	2123	0.366
TTG168-L	Mastic	1182	0.365
TTG074-L	Bromobenzene	2057	0.364
TTG016-L(C)	Pentachlorophenol	1968	0.363
TTG189-L	TTG4: A) CCl4, B) Ccl4 (TTG4(1+1))	1161	0.36
TTG157-L	Valproic acid sodium salt	2072	0.357
TTG202-L	TTG4: A) Clofibrate, B) Clofibrate (TTG4(4+1))	848	0.357
TTG162-L	Sesame seed oil unsaponified matter	1373	0.356
TTG147-L	Estragole	813	0.355
TTG066-L	Methoprene	821	0.354
TTG090-L	Pregnenolone Carbonitrile	1277	0.352
TTG149-L	Valproic acid sodium salt x Aspirin	1187	0.35
TTG182-L	Imidacloprid	1427	0.347
TTG183-L	Bisphenol A (corn oil)	858	0.339
TTG087-L	Pyriproxyfen	905	0.334
TTG056-L	3-methylcholanthrene	1229	0.333
TTG043-L	Testosterone propionate	666	0.332
TTG094-L	Aspirin	1188	0.332
TTG093-L	AraC	873	0.329
TTG047-L	Bisphenol A (PLD)	631	0.327
TTG194-L	TTG4: A) Valproic acid sodium salt, B) Valproic acid sodium salt (TTG4(2+1))	2021	0.326
TTG053-L	Ethynyl estradiol (PLD)	1665	0.323
TTG199-L	Black No.401	627	0.323
TTG070-L	Formaldehyde	302	0.322
TTG154-L	Sodium Dehydroacetate	1558	0.322
TTG124-L	Vat Red I	725	0.32
TTG046-L	Levothyroxine	1143	0.316
TTG089-L	Rifampicin	641	0.315
TTG122-L	CoenzymeQ10(14day)	1179	0.314
TTG020-L	TCDD(2,3,7,8-Tetrachlorodibenzo-p-Dioxin)	1147	0.313
TTG061-L	Paraquat dichloride	993	0.313
TTG132-L	Curcumin	1471	0.313
TTG155-L	Aluminum ammonium sulfate	851	0.313
TTG086-L	Coenzyme Q10	1429	0.311
TTG156-L	Food Red No.104	1276	0.311
TTG173-L	TCDD/AhRKO	2432	0.311
TTG165-L	Chlorpyrifos	763	0.31
TTG201-L	TTG4: A) Clofibrate, B) Clofibrate (TTG4(2+1))	818	0.31
TTG031-L	2-Chloro-4,6-dimethylaniline	1093	0.309
TTG060-L	Forskolin	508	0.307
TTG057-L	Indigo	400	0.306
TTG137-L	alpha-Lipoic Acid	712	0.304

Percellome Explorer ver. 0.5.0 : PDBEx_RSort_Expand_H_G2_AP_Std-Av@
Target Prj: vs TTG206-L // BTAZ3864(CoCAM 2)
Denominator: Target * Candidate

Name	Condition	Num	Cor
TTG206-L	BTAZ3864(CoCAM 2)	9318	1.073
TTG098-L	DEHP	3595	0.68
TTG118-L	Clofibrate x Clofibrate	1899	0.578
TTG205-L	BTAZ3846(CoCAM 1)	6508	0.57
TTG044-L	Clofibrate	1708	0.553
TTG104-L	MEHP	2714	0.535
TTG141-L	Tributyltin chloride x Clofibrate	2182	0.533
TTG129-L	CCl4 x Clofibrate	1441	0.527
TTG120-L	Clofibrate x PCN	1363	0.514
TTG016-L	Pentachlorophenol	1418	0.509
TTG200-L	TTG4: A) Clofibrate, B) Clofibrate (TTG4(1+1))	950	0.503
TTG144-L	Tributyltin chloride x Phenobarbital	1343	0.497
TTG151-L	Valproic acid sodium salt x Valproic acid sodium salt	1650	0.489
TTG202-L	TTG4: A) Clofibrate, B) Clofibrate (TTG4(4+1))	838	0.465
TTG168-L	Mastic	1105	0.449
TTG195-L	TTG4: A) Valproic acid sodium salt, B) Valproic acid sodium salt (TTG4(4+1))	1764	0.446
TTG193-L	TTG4: A) Valproic acid sodium salt, B) Valproic acid sodium salt (TTG4(1+1))	1405	0.445
TTG162-L	Sesame seed oil unsaponified matter	1265	0.432
TTG204-L	Red No.225	1644	0.42
TTG032-L	3-Amino-1H-1,2,4-triazole	2568	0.416
TTG147-L	Estragole	716	0.411
TTG041-L	Valproic acid sodium salt	2166	0.407
TTG201-L	TTG4: A) Clofibrate, B) Clofibrate (TTG4(2+1))	796	0.397
TTG073-L	Toluene	1099	0.396
TTG016-L(C)	Pentachlorophenol	1627	0.395
TTG090-L	Pregnenolone Carbonitrile	1088	0.394
TTG157-L	Valproic acid sodium salt	1742	0.394
TTG019-L	2-Vinylpyridine	754	0.392
TTG149-L	Valproic acid sodium salt x Aspirin	995	0.386
TTG183-L	Bisphenol A (corn oil)	740	0.385
TTG199-L	Black No.401	567	0.385
TTG194-L	TTG4: A) Valproic acid sodium salt, B) Valproic acid sodium salt (TTG4(2+1))	1811	0.384
TTG066-L	Methoprene	674	0.382
TTG043-L	Testosterone propionate	582	0.381
TTG037-L	Phenobarbital	1975	0.38
TTG139-L	Indigo Carmine	852	0.374
TTG020-L	TCDD(2,3,7,8-Tetrachlorodibenzo-p-Dioxin)	1036	0.372
TTG047-L	Bisphenol A (PLD)	539	0.367
TTG136-L	Phytol	1603	0.364
TTG189-L	TTG4: A) CCl4, B) Ccl4 (TTG4(1+1))	883	0.361
TTG070-L	Formaldehyde	256	0.36
TTG031-L	2-Chloro-4,6-dimethylaniline	962	0.358
TTG182-L	Imidacloprid	1122	0.358
TTG046-L	Levothyroxine	982	0.357
TTG132-L	Curcumin	1239	0.347
TTG060-L	Forskolin	436	0.346
TTG154-L	Sodium Dehydroacetate	1274	0.346
TTG187-L	Violet No.201	674	0.346
TTG124-L	Vat Red I	594	0.345
TTG155-L	Aluminum ammonium sulfate	695	0.337
TTG074-L	Bromobenzene	1441	0.336
TTG062-L(C)	Dexamethasone	962	0.335
TTG093-L	AraC	672	0.333
TTG137-L	alpha-Lipoic Acid	586	0.329
TTG086-L	Coenzyme Q10	1145	0.328
TTG057-L	Indigo	324	0.326
TTG094-L	Aspirin	887	0.326
TTG015-L	4-amino-2,6-dichlorophenol	297	0.325
TTG188-L	Violet No.401	429	0.323
TTG029-L	2-Aminomethylpyridine	237	0.322
TTG087-L	Pyriproxyfen	664	0.322
TTG056-L	3-methylcholanthrene	897	0.32
TTG091-L	Azacytidine	505	0.32

別添 4

Ⅱ．　研究成果の刊行に関する一覧表

別添4

研究成果の刊行に関する一覧表

雑誌

発表者氏名	論文タイトル名	発表誌名	巻名	ページ	出版年
Janesick A, Nguyen TT, Aisaki K, Igarashi K, Kitajima S, Chandraratna RA, Kanno J, Blumberg B.	Active repression by RARγ signaling is required for vertebrate axial elongation.	Development	141 (11)	2260 - 2270	2014
Tanaka M, Aisaki K, Kitajima S, Igarashi K, Kanno J and Nakamura T	Gene expression response to EWS–FLI1 in mouse embryonic cartilage.	Genomics Data	2	296 - 298	2014
Tanaka M, Yamazaki Y, Kanno Y, Igarashi K, Aisaki K, Kanno J, Nakamura T.	Ewing's sarcoma precursors are highly enriched in embryonic osteochondrogenic progenitors.	J Clin Invest.	124 (7)	3061 - 3074	2014
Maria Marti-Solano, Ewan Birney, Antoine Bril, Oscar Della Pasqua, Hiroaki Kitano, Barend Mons, Ioannis Xenarios and Ferran Sanz	Integrative knowledge management to enhance pharmaceutical R&D.	Nature Reviews Drug Discovery	13 (4)	239 - 240	2014
Yoshiyuki ASAI; Takeshi ABE, Hideki OKA, Masao OKITA, Ken-ichi HAGIHARA, Samik GHOSH, Yukiko MATSUOKA, Yoshihisa KURACHI, Taishin NOMURA, Hiroaki KITANO	A Versatile Platform for Multilevel Modeling of Physiological Systems: SBML-PHML Hybrid Modeling and Simulation.	ABE Advanced Biomedical Engineering	3	50 - 58	2014
Tokiko Watanabe, Eiryo Kawakami, Jason E. Shoemaker, Tiago J.S. Lopes, Yukiko Matsuoka, Yuriko Tomita, Hiroko Kozuka-Hata, Takeo Gorai, Tomoko Kuwahara, Eiji Takeda, Atsushi Nagata, Ryo Takano, Maki Kiso, Makoto Yamashita, Yuko Sakai-Tagawa, Hiroaki Katsura, Naoki Nonaka,	Influenza Virus-Host Interactome Screen as a Platform for Antiviral Drug Development	Cell Host & Microbe	16 (6)	795 - 805	2014

Hiroko Fujii, Ken Fujii, Yukihiko Sugita, Takeshi Noda, Hideo Goto, Satoshi Fukuyama, Shinji Watanabe, Gabriele Neumann, Masaaki Oyama, Hiroaki Kitano, and Yoshihiro Kawaoka					
Jablonska Agnieszka and Natalia Polouliakh	In silico discovery of novel transcription factors regulated by mTOR pathway activities	Frontier in Cell and Developmental Biology ISSN: 2296-634X DOI:10.3389/fcell.	2 (23)	1 - 9	2014
Kanno J, Aisaki K, Igarashi K, Kitajima S, Matsuda N, Morita K, Tsuji M, Moriyama N, Furukawa Y, Otsuka M, Tachihara E, Nakatsu N, Kodama Y.	Oral administration of pentachlorophenol induces interferon signaling mRNAs in C57BL/6 male mouse liver.	J Toxicol Sci.	38 (4)	643 - 654	2013
Fujimoto N, Takagi A, Kanno J.	Neonatal exposure to 2,3,7,8-tetrachlorodibenze-p-dioxin increases the mRNA expression of prostatic proteins in C57BL mice.	J Toxicol Sci.	38 (2)	279 - 283	2013
Hase T, Ghosh S, Yamanaka R, Kitano H.	Harnessing Diversity towards the Reconstructing of Large Scale Gene Regulatory Networks.	PLOS Computational Biology	9 (11)	1 - 16	2013
Yukiko Matsuoka; Hiromi Matsumae; Manami Katoh; Amie J Eisfeld; Gabriele Neumann; Takeshi Hase; Samik Ghosh; Jason E Shoemaker; Tiago JS Lopes; Tokiko Watanabe; Shinji Watanabe; Satoshi Fukuyama; Hiroaki Kitano; and Yoshihiro Kawaoka.	A comprehensive map of the influenza A virus replication cycle.	BMC Systems Biology	7 (97)	1 - 18	2013
Yamashita Fumiyoshi; Yukako Sasa; Shuya Yoshida; Akihiro Hisaka;	Modeling of Rifampicin-Induced	PLOS ONE	8 (9)	1 -	2013

Yoshiyuki Asai; Hiroaki Kitano; Mitsuru Hashida, Hiroshi Suzuki.	CYP3A4 Activation Dynamics for the Prediction of Clinical Drug-Drug Interactions from In Vitro Data.			11	
Kazuhiro A. Fujita; Marek Ostaszewski; Yukiko Matsuoka; Samik Ghosh; Enrico Glaab; Christophe Trefois; Isaac Crespo; Thanneer M. Perumal; Wiktor Jurkowski; Paul M. A. Antony; Nico Diederich; Manuel Buttini; Akihiko Kodama; Venkata P. Satagopam; Serge Eifes; Antonio del Sol; Reinhard Schneider; Hiroaki Kitano; Rudi Balling.	Integrating Pathways of Parkinson's Disease in a Molecular Interaction Map.	Molecular Neurobiology	49	88 - 102	2014
Naito T, Yatsuhashi A, Kaji N, Ando T, Sato, K, Moriya H, Kitano H, Yasui T, Tokeshi M, Baba Y.	Parallel Real-Time PCR on a Chip for Genetic Tug-of-War (gTOW) Method.	Analytical Sciences	29 (3)	367 - 371	2013
Koji Makanae; Reiko Kintaka; Takashi Makino; Hiroaki Kitano; and Hisao Moriya.	Identification of dosage-sensitive genes in Saccharomyces cerevisiae using the genetic tug-of-war method.	Genome Research	23	300 - 311	2013
Natalia Polouliakh	Reprogramming resistant genes: in-depth comparison of gene expressions among iPS, ES and somatic cells.	Frontier of Physiology	4 (7)	1 - 9	2013
Abe S, Kurata M, Suzuki S, Yamamoto K, Aisaki K, Kanno J, Kitagawa M.	Minichromosome maintenance 2 bound with retroviral Gp70 is localized to cytoplasm and enhances DNA-damage-induced apoptosis.	PLoS One	7 (6)	e40129	2012
Swedenborg E, Kotka M, Seifert M, Kanno J, Pongratz I, Rüegg J.	The aryl hydrocarbon receptor ligands 2,3,7,8-tetrachlorodibenzo-p-dioxin and 3-methylcholanthrene	Mol Cell Endocrinol.	362 (1-2)	39 - 47	2012

	regulate distinct genetic networks.				
Igarashi K, Kitajima S, Aisaki K, Tanemura K, Taquahashi Y, Moriyama N, Ikeno E, Matsuda N, Saga Y, Blumberg B, Kanno J.	Development of humanized steroid and xenobiotic receptor mouse by homologous knock-in of the human steroid and xenobiotic receptor ligand binding domain sequence.	J Toxicol Sci.	37 (2)	373 - 380	2012
Crespo, I.; Roomp, K.; Jurkowski, W.; Kitano, H.; del Sol, A.	Gene regulatory network analysis supports inflammation as a key neurodegeneration process in prion disease.	BMC Systems Biology	6 (132)	1 - 12	2012
Shoemaker, J.; Fukuyama, S.; Eisfeld, A. J.; Muramoto, Y.; Watanabe, S.; Watanabe, T.; Matsuoka, Y.; Kitano, H.; Kawaoka, Y.	Integrated network analysis reveals a novel role for the cell cycle in 2009 pandemic influenza virus-induced inflammation in macaque lungs.	BMC Systems Biology	6 (117)	1 - 14	2012
Shoemaker, J. E., Lopes, T. J., Ghosh, S., Matsuoka, Y., Kawaoka, Y., Kitano, H.	CTen : a web-based platform for identifying enriched cell types from heterogeneous microarray data.	BMC Genomics	13 (460)	1 - 11	2012
Martijn P. van Iersel, Alice C. Villeger, Tobias Czauderna, Sarah E. Boyd, Frank T. Bergmann, Augustin Luna, Emek Demir, Anatoly Sorokin, Ugur Dogrusoz, Yukiko Matsuoka, Akira Funahashi, Mirit I. Aladjem, Huaiyu Mi, Stuart L. Moodie, Hiroaki Kitano Nicolas Le Novere, and Falk Schreiber.	Software support for SBGN maps: SBGN-ML and LibSBGN.	Bioinformatics	28 (15)	2016 - 2021	2012
Carl-Fredrik Tiger, Falko Krause, Gunnar Cedersund, Robert Palmér, Edda Klipp, Stefan Hohmann, Hiroaki Kitano and Marcus Krantz.	A framework for mapping, visualisation and automatic model creation of signal-transduction networks.	Molecular Systems Biology.	8 (578)	1 - 20	2012

Ⅲ.　研究成果の刊行物・別刷

© 2014. Published by The Company of Biologists Ltd | Development (2014) 141, 2260-2270 doi:10.1242/dev.103705

RESEARCH ARTICLE

Active repression by RARγ signaling is required for vertebrate axial elongation

Amanda Janesick[1], Tuyen T. L. Nguyen[1], Ken-ichi Aisaki[2], Katsuhide Igarashi[2], Satoshi Kitajima[2], Roshantha A. S. Chandraratna[3], Jun Kanno[2] and Bruce Blumberg[1,4,*]

ABSTRACT

Retinoic acid receptor gamma 2 (RARγ2) is the major RAR isoform expressed throughout the caudal axial progenitor domain in vertebrates. During a microarray screen to identify RAR targets, we identified a subset of genes that pattern caudal structures or promote axial elongation and are upregulated by increased RAR-mediated repression. Previous studies have suggested that RAR is present in the caudal domain, but is quiescent until its activation in late stage embryos terminates axial elongation. By contrast, we show here that RARγ2 is engaged in all stages of axial elongation, not solely as a terminator of axial growth. In the absence of RA, RARγ2 represses transcriptional activity *in vivo* and maintains the pool of caudal progenitor cells and presomitic mesoderm. In the presence of RA, RARγ2 serves as an activator, facilitating somite differentiation. Treatment with an RARγ-selective inverse agonist (NRX205099) or overexpression of dominant-negative RARγ increases the expression of posterior Hox genes and that of marker genes for presomitic mesoderm and the chordoneural hinge. Conversely, when RAR-mediated repression is reduced by overexpressing a dominant-negative co-repressor (c-SMRT), a constitutively active RAR (VP16-RARγ2), or by treatment with an RARγ-selective agonist (NRX204647), expression of caudal genes is diminished and extension of the body axis is prematurely terminated. Hence, gene repression mediated by the unliganded RARγ2–co-repressor complex constitutes a novel mechanism to regulate and facilitate the correct expression levels and spatial restriction of key genes that maintain the caudal progenitor pool during axial elongation in *Xenopus* embryos.

KEY WORDS: Active repression, Axial elongation, Chordoneural hinge, Posterior Hox, Presomitic mesoderm, Retinoic acid receptor

INTRODUCTION

Repression mediated through unliganded retinoic acid receptors (RARs) is an important yet understudied function exhibited by nuclear receptors (reviewed by Weston et al., 2003). Although RA plays a major role in patterning the hindbrain, retina, placodes and somites, its absence is crucial for the development of structures found at the head and tail of the embryo. RARs exhibit basal repression in the absence of ligand, binding constitutively to their targets, recruiting co-repressors, and actively repressing the basal transcriptional machinery (Chen and Evans, 1995). When ligand is present, co-repressors are replaced by co-activators and target genes are transcribed (Chakravarti et al., 1996).

We previously demonstrated that repression mediated through unliganded RARs was important for anterior neural patterning, establishing a novel role for RAR as a repressor *in vivo* (Koide et al., 2001). Overexpression of a dominant-negative RARα expanded anterior and midbrain markers caudally and shifted somitomeres rostrally (Blumberg et al., 1997; Moreno and Kintner, 2004). Exogenous RA, constitutively active RARα or derepression of RARα produced the opposite effect: severe anterior truncations, diminished anterior markers, and anteriorly shifted midbrain and hindbrain markers. Stabilization of co-repressors resulted in enhanced anterior neural structures and posteriorly shifted mid/hindbrain markers (Koide et al., 2001).

Axial elongation requires continual replenishing of bipotential caudal progenitor cells (maintained by Wnt and FGF signaling, but inhibited by RA) that give rise to notochord, neural tube and somites (Cambray and Wilson, 2002; Davis and Kirschner, 2000). The most stem-like cells are located in the chordoneural hinge (CNH), where the posterior neural plate overlies the caudal notochord (Beck and Slack, 1998). Cells from the CNH contribute to presomitic mesoderm (PSM), which supplies committed somitic precursor cells to the rostral determination wavefront (reviewed by Dequeant and Pourquie, 2008). PSM is initially homogenous and unorganized [expressing *Mesogenin1* (*Msgn1*) and *Tbx6*], then becomes patterned into somitomeres marked by *Thylacine2* (*Thyl2*) and *Ripply2* (reviewed by Dahmann et al., 2011). Epithelialization of presomitic domains results in mature somites (Nakaya et al., 2004).

RA is well known to function in the trunk, where it promotes differentiation of PSM into somitomeres (Moreno and Kintner, 2004). By contrast, RA is actively metabolized and cleared by CYP26A1 in the caudal region (Fujii et al., 1997). Treatment with RA leads to loss of posterior structures (Sive et al., 1990); *Cyp26a1*$^{-/-}$ mice exhibit posterior truncations and homeotic vertebral transformations (Abu-Abed et al., 2001; Sakai et al., 2001). Exposing embryos to RA inhibits proliferation of axial progenitor cells in CNH and PSM, leading to axial truncation from premature exhaustion of the progenitor pool (Gomez and Pourquie, 2009). Therefore, RA is normally excluded from unsegmented mesenchyme in PSM and the CNH. RARγ is expressed at high levels throughout the entire caudal region, including CNH and PSM (Mollard et al., 2000; Pfeffer and De Robertis, 1994), yet, based on *Cyp26a1* expression, RA is absent (de Roos et al., 1999). The physiological significance of RARγ expression in the embryonic posterior is uncertain. RARγ might function to terminate the body axis at late stages by inducing apoptosis (Olivera-Martinez et al., 2012), but that model would not explain the strong expression of RARγ observed at neurula, continuing through tailbud stages, despite the apparent absence of RA.

[1]Department of Developmental and Cell Biology, 2011 Biological Sciences 3, University of California, Irvine, CA 92697-2300, USA. [2]Division of Cellular and Molecular Toxicology, Biological Safety Research Center, National Institute of Health Sciences, 1-18-1 Kamiyoga, Setagaya-ku, Tokyo 158-8501, Japan. [3]IO Therapeutics, Santa Ana, CA 92705-5851, USA. [4]Department of Pharmaceutical Sciences, University of California, Irvine, CA 92697-2300, USA.

*Author for correspondence (blumberg@uci.edu)

Received 29 September 2013; Accepted 27 March 2014

Development (2014) 141, 2260-2270 doi:10.1242/dev.103705

Rarγ2 skirts the posterior edge of the determination wavefront and is co-expressed with PSM, CNH and posterior Hox markers. We hypothesized that *Rarγ2* serves a dual function: as an activator in somite differentiation but a repressor in the maintenance of PSM and the caudal progenitor pool. Loss of RARγ2 severely shortens the embryo body axis and inhibits somitogenesis. Loss of RARγ2 expands the anterior border of PSM expression near the wavefront (where activation is lost), but diminishes the expression domain of caudal PSM and posterior Hox genes (where repression is lost). Increasing RAR-mediated repression expands the expression of posterior Hox, PSM and CNH markers, creating smaller somitomere domains via an indirect, 'repressing a repressor' mechanism. Relief of repression results in a truncated body axis with decreased PSM and CNH markers. Axial extension and segmentation in vertebrates relies on the maintenance of unsegmented PSM mesenchyme and replenishing of caudal progenitor cells. Our data show that RARγ2 plays a crucial role in this process, repressing target genes to maintain PSM and caudal progenitors in the absence of RA, while activating others to promote somitogenesis in the presence of RA.

RESULTS

Posterior Hox, PSM and CNH genes are upregulated by RAR inverse agonist

We showed previously that active repression of RAR target genes by unliganded RAR is required for head formation (Koide et al., 2001). Treatment with the pan-RAR inverse agonist AGN193109 increased the expression of genes involved in patterning anterior neural structures, whereas treatment with pan-RAR agonist TTNPB decreased the expression of anterior marker and cement gland-specific genes (Koide et al., 2001), revealing a set of genes specifically upregulated/downregulated by TTNPB (Arima et al., 2005). Validation studies identified a subset upregulated by AGN193109. We hypothesized that active repression by unliganded RARs is biologically important and designed an experiment to identify genes upregulated or downregulated by modulating repression. Percellome analysis (Kanno et al., 2006) quantified the copy number per embryo of all genes represented on Affymetrix *Xenopus* microarray v1.0. Among these we identified a collection of genes linked to the maintenance of caudal axial progenitors that were downregulated by TTNPB and upregulated by AGN193109 (Table 1). RAR-mediated repression upregulates the steady-state expression of posterior Hox paralogs 9-13 and genes found in both unsegmented PSM and CNH. Thus, we hypothesized that RAR is a repressor required for axial elongation.

Xenopus RARs repress basal transcription in the absence of ligand

The ability of unliganded RARs to behave as repressors is well documented, although not all human receptor subtypes can recruit co-repressors (e.g. SMRT) in the absence of ligand (Wong and Privalsky, 1998). We tested the ability of *Xenopus* RAR (xRAR) subtypes to repress basal activity of a luciferase-dependent reporter using the GAL4-RAR system (supplementary material Fig. S1D-F) (Blumberg et al., 1996). *Xenopus* RARα, RARβ and RARγ suppressed basal activity *in vitro* and *in vivo* (supplementary material Fig. S1A,C), whereas human RARβ and RARγ did not (supplementary material Fig. S1B). Thus, xRARs can function as repressors in the absence of ligand.

Rarγ2 is expressed in the PSM and CNH but is mostly absent from the trunk

Whole-mount *in situ* hybridization (WISH) revealed that *Rarγ2* is the predominant isoform expressed in the *Xenopus* embryonic posterior (supplementary material Fig. S2A). In late neurula and early tailbud stage embryos, *Rarγ2* is strongly expressed in the anterior and posterior, but almost undetectable in the trunk. *Rarγ2* expression later becomes pronounced in the tail and head, particularly in hyoid, branchial and mandibular neural crest. *Rarγ1* is expressed similarly. QPCR analysis revealed that *Rarγ2* is 1000- to 4000-fold more abundant than *Rarγ1* at stages 10-22, and 100- to 400-fold more abundant at all other stages analyzed (supplementary material Fig. S2B). Subsequent experiments utilized *Rarγ2*-selective reagents. We conclude that *Rarγ2* is the predominant isoform expressed in the posterior region of embryos.

Rarγ2 is expressed where RA is probably absent (owing to CYP26A1 expression). Key posterior genes were upregulated by AGN193109. We hypothesized that RARγ2 posterior to the wavefront is a repressor, maintaining unsegmented PSM and the progenitor cell pool required for axial elongation. We used double WISH to compare the expression of *Rarγ2* with that of *Hoxc10*, an important member of the Abd-B Hox gene family promoting caudal development over thorax (Lamka et al., 1992). *Rarγ2* expression completely overlaps caudal *Hoxc10* expression (Fig. 1E,H) but not the anteriormost neural or lateral plate expression of *Hoxc10* (Fig. 1E,H). These data position

Table 1. Percellome analysis reveals that posterior Hox, PSM and CNH markers are upregulated by RAR inverse agonist

Unigene	109 (fold)	*P*	TTN (fold)	*P*	Symbol	Gene name	Cat
Xl.72193	3.57	2.11×10^{-3}	0.19	5.77×10^{-4}	*Hoxc13*	Homeobox C13	PP
Xl.266	3.47	4.26×10^{-3}	0.12	2.26×10^{-4}	*Hoxa11*	Homeobox A11	PP
Xl.21864	3.15	2.03×10^{-3}	0.22	2.68×10^{-4}	*Hoxc10*	Homeobox C10	PP
Xl.72292	3.02	7.32×10^{-3}	0.16	1.62×10^{-4}	*Hoxd9*	Homeobox D9	PP
Xl.9560	2.73	9.74×10^{-4}	0.40	5.98×10^{-3}	*Hoxa9*	Homeobox A9	PP
Xl.12067	2.80	8.05×10^{-3}	0.18	2.51×10^{-5}	*Esr2*	Enhancer of Split related 2	PSM
Xl.29033	2.79	9.31×10^{-4}	0.26	1.62×10^{-5}	*Esr9*	Enhancer of Split related 9	PSM
Xl.78953	2.90	4.29×10^{-4}	0.37	2.68×10^{-3}	*Tbx6*	T-box gene Tbx6	PSM
Xl.483	2.53	4.18×10^{-3}	0.17	3.36×10^{-8}	*Msgn1*	Mesogenin 1	PSM
Xl.14524	2.32	2.76×10^{-2}	0.42	1.46×10^{-2}	*Esr5*	Enhancer of Split related 5	PSM
Xl.933	2.49	4.46×10^{-2}	0.40	2.73×10^{-2}	*xBra3*	T2, Brachyury homolog	CNH
Xl.1066	2.44	4.31×10^{-2}	0.34	2.09×10^{-3}	*xNot*	Notochord homeobox	CNH
Xl.457	3.10	1.37×10^{-3}	0.02	2.81×10^{-7}	*Derriere*	Growth differentiation factor 3	NC
Xl.16206	2.43	7.64×10^{-3}	0.27	2.35×10^{-6}	*Pnp*	Purine nucleoside phosphorylase	NC

Blastula stage embryos were soaked in 1 μM RAR agonist TTNPB (TTN), 1 μM RAR inverse agonist AGN193109 (109) or vehicle control (0.1% ethanol) until harvesting at stage 18. Cat, expression category: PP, posterior patterning; PSM, presomitic mesoderm; CNH, chordoneural hinge; NC, expression not characterized. Fold induction or reduction is relative to control vehicle. *P*-values were generated using CyberT.

Development (2014) 141, 2260-2270 doi:10.1242/dev.103705

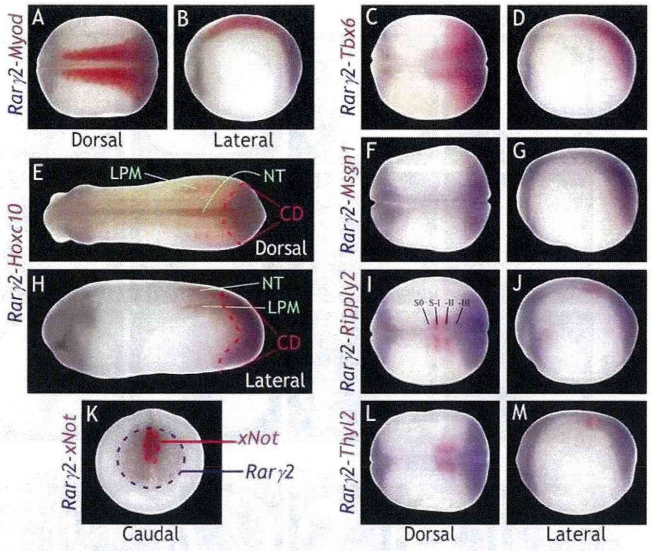

Fig. 1. Double WISH reveals the spatial relationship between *Rarγ2* and posterior Hox, PSM and CNH genes. (A-M) *Rarγ2* is stained with BM Purple and the other genes are stained with Fast Red. *Rarγ2* is caudal to *Myod* and *Tbx6* (A-D), but synexpressed with *Msgn1* (F,G) in neurula stage *Xenopus* embryos. (E,H) *Rarγ2* is synexpressed with the caudal domain (CD) of *Hoxc10* but not with neural tube (NT) or lateral plate mesoderm (LPM) of *Hoxc10* in tailbud stage embryos. *Rarγ2* overlaps with S–III domains of *Ripply2* (I,J) and *Thyl2* (L,M) expression, but not with more anterior somitomeres (S–II, S–I, S0). (K) *Rarγ2* overlaps with *xNot* expression in neurula stage embryos. Dorsal and lateral views shown with anterior to the left, except in K (caudal view with dorsal at top).

Rarγ2 as a potential regulator of posterior Hox genes and the caudal body plan.

We next defined the anterior limit of *Rarγ2* expression relative to the determination wavefront. *Myod* is a general muscle marker abutting and partially overlapping *Rarγ2* expression (Fig. 1A,B). *Thyl2* and *Ripply2* mark somitomeres, which are prepatterned PSM domains containing non-epithelialized, immature somites (Tam et al., 2000). *Thyl2* and *Ripply2* are only expressed in newly forming somitomeres and are assigned negative Roman numerals (S–I, S–II, etc.) versus mature somites (SI, SII, etc.) (Pourquie and Tam, 2001). *Msgn1* (Buchberger et al., 2000) is expressed caudal to *Thyl2* and *Ripply2*, marking non-patterned PSM-containing cells committed to the somitic fate (Nowotschin et al., 2012). *Tbx6* is also expressed in PSM, but unlike *Msgn1* its expression domain overlaps with somitomeres (Hitachi et al., 2008). *Rarγ2* and *Msgn1* are synexpressed at neurula (Fig. 1F,G) and tailbud (supplementary material Fig. S3) stages; *Tbx6* expression overlaps *Rarγ2* but extends rostrally beyond the *Rarγ2* domain (Fig. 1C,D; supplementary material Fig. S3). Anterior expression of *Rarγ2* mRNA ends at an RA-responsive region (supplementary material Fig. S4), coinciding with the most posterior somitomere domain (S–III) of *Thyl2* or *Ripply2* (Fig. 1I-M), thus skirting the posterior edge of the wavefront.

xNot, a notochord marker that regulates trunk and tail development, is concentrated in the extreme posterior notochord and floor plate by late neurula (von Dassow et al., 1993) and is often employed as a CNH marker in *Xenopus* (Beck and Slack, 1998) to reveal the location of bipotential stem cells (Cambray and Wilson, 2007; Takemoto et al., 2011). *xNot* is co-expressed with *Rarγ2* (Fig. 1K), agreeing with data suggesting that *Rarγ2* is present in CNH (Pfeffer and De Robertis, 1994). The double WISH data are consistent with *Rarγ2* functioning as an activator near where RA is present at the wavefront, yet as a repressor where it coincides with *Msgn1*, *xNot* and *Cyp26a1*.

RARγ-selective chemicals modulate activation or repression by RARγ

To separate the effects of RARγ in the posterior from RARα in the trunk, we characterized RARγ-selective agonist NRX204647 (4647) (Shimono et al., 2011; Thacher et al., 2000) and RARγ-selective inverse agonist NRX205099 (5099) (Tsang et al., 2003) in *Xenopus* embryos. Like AGN193109, 5099 is an inverse agonist, reducing RARγ signaling activity below basal levels by stabilizing the co-repressor complex bound to RARγ. Embryos treated with 1 μM agonist 4647 become primarily trunk (no head or tail structure), while 0.1 μM perturbs axial elongation (supplementary material Fig. S5), producing anterior truncations characteristic of RAR activators (Sive et al., 1990). Inverse agonist 5099 at 1 μM delayed development, producing enlarged heads and shortened trunks; half the dose elicited similar but weaker phenotypes, with effects absent at 0.1 μM (supplementary material Fig. S5). Treating neurula embryos significantly reduced severity but did not eliminate the phenotype (supplementary material Fig. S5).

To test the effects of these chemicals *in vivo* without interference from endogenous RARs, we mutated the DNA-binding specificity of a full-length RAR, $RAR^{EGCKG\rightarrow GSCKV}$. The mutant receptor recognizes a mutant TK-luc reporter, $(RXRE^{1/2}\text{-}GRE^{1/2})\times 4$ TK-luc, to which endogenous RARs do not bind (Klein et al., 1996). In transient transfection assays, 4647 selectively activated RARγ at doses below 0.1 μM (supplementary material Fig. S6A). Similarly, 5099 selectively antagonized 10 nM 9-cis RA activation of RARγ below 0.1 μM (supplementary material Fig. S6B). We conclude that 4647 and 5099 behave as subtype-selective ligands to activate or repress RARγ.

RARγ-selective chemicals affect posterior Hox genes, PSM and somitomeres

We hypothesized that 4647 treatment of embryos would decrease posterior Hox gene expression and markers of PSM, whereas 5099 would produce the opposite effect. Microarray analysis (Table 1) revealed that *Hoxc13* and *Hoxc10* expression was upregulated by inverse agonist AGN193109 and downregulated by agonist TTNPB. We infer that increased expression of *Hoxc13* and *Hoxc10* results from RAR repressing the expression of a repressor of their expression. The expression pattern of *Hoxc13* (supplementary material Fig. S7) was not previously characterized.

We began soaking embryos in RARγ-selective doses of 4647, 5099 or vehicle control after gastrulation (stage 12.5) to focus on axial elongation. Treatment with 10 nM 4647 resulted in diminished caudal structures at stage 40 (supplementary material Fig. S5), reducing expression domains of *Hoxc10*, *Hoxd10* and *Hoxc13* (Fig. 2A-C). Conversely, treatment with 0.5 μM 5099 expanded their neural and lateral domains (Fig. 2A-C). To determine short-term effects of chemical treatments, we soaked embryos for 1 h at various stages and evaluated *Hoxc10* expression (supplementary material Fig. S8) and that of *Tbx6* (not shown) at stage 22. Repression by 5099 is required at early neurula, whereas activation by 4647 is required at mid- and late neurula stages for expected expansion and reduction, respectively, of *Hoxc10* expression (supplementary material Fig. S8). Higher, non-receptor-selective doses exacerbated effects on posterior Hox genes (supplementary material Fig. S9), suggesting that RARγ2 is the primary mediator. *Hoxc10* nearly abuts *Krox20*, demonstrating trunk shortening in 5099-treated embryos (supplementary material Fig. S9G,H). High

Development (2014) 141, 2260-2270 doi:10.1242/dev.103705

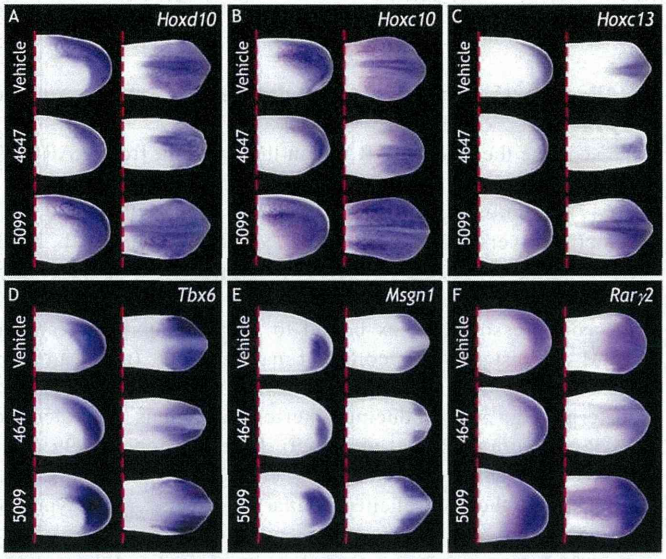

Fig. 2. Posterior Hox and PSM markers are reduced by RARγ-selective agonist and expanded by RARγ-selective inverse agonist. (A-F) WISH from embryos treated post-gastrulation (stage 12.5) with 10 nM 4647, 0.5 μM 5099 or vehicle (0.1% ethanol). Dashed red line represents half the embryo axis. 4647 diminishes and 5099 expands the expression of (A) *Hoxd10* (4647, 16/16; 5099, 17/17 embryos), (B) *Hoxc10* (4647, 14/14; 5099, 21/21), (C) *Hoxc13* (4647, 12/12; 5099, 16/16), (D) *Tbx6* (4647, 11/12; 5099, 17/17), (E) *Msgn1* (4647, 15/15; 5099, 14/14), and (F) *Rarγ2* (4647, 15/15; 5099, 9/9) relative to control vehicle. Embryos shown in lateral or dorsal view at tailbud stage, anterior to left.

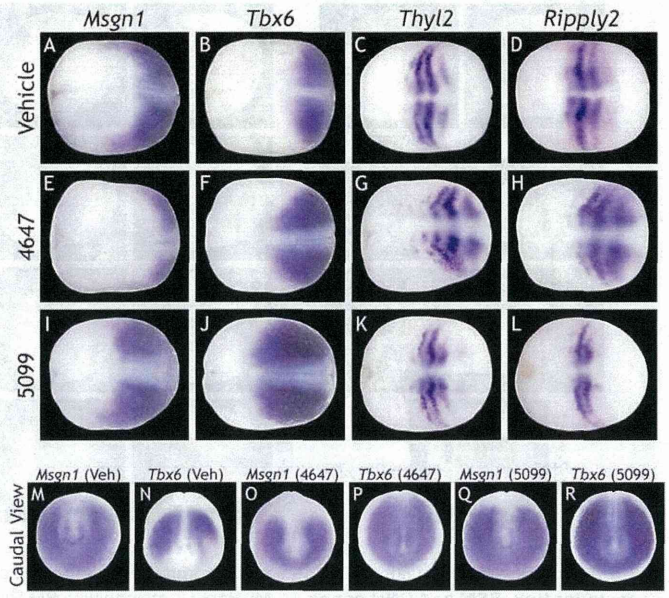

Fig. 3. PSM markers are modulated by RARγ-selective agonist and inverse agonist. (A-R) WISH from embryos treated post-gastrulation (stage 12.5) with 10 nM 4647, 0.5 μM 5099 or vehicle (0.1% ethanol). (A-D) Control expression of *Msgn1*, *Tbx6*, *Thyl2* and *Ripply2*. (E) *Msgn1* expression diminished by 4647 treatment (17/17 embryos). (F) *Tbx6* expression expanded by 4647 treatment (22/22). (G,H) Somitomere domains of *Thyl2* (19/19) and *Ripply2* (17/17) are thicker and posteriorly expanded. (I,J) *Msgn1* (17/17) and *Tbx6* (13/13) expression expanded by 5099 treatment. (K,L) Somitomere domains of *Thyl2* (15/17) and *Ripply2* (26/26) are fewer and thinner. Embryos are shown in dorsal view at neurula stage, anterior to left. (M-R) Caudal views of *Msgn1* and *Tbx6*.

doses of 4647 create embryos lacking anterior and posterior structures, as indicated by the absence of mid/hindbrain markers *En2* and *Krox20* and of posterior gene *Hoxc10* (supplementary material Fig. S9C-F).

Msgn1 and *Tbx6* were upregulated by inverse agonist and downregulated by agonist in the microarray analysis (Table 1). *Msgn1* and *Tbx6* domains were reduced at tailbud stages by post-gastrulation treatment of embryos with 4647, whereas expression was expanded in embryos treated with inverse agonist 5099 (Fig. 2D,E). However, in neurula stage embryos, 4647 reduced *Msgn1* expression while *Tbx6* expression was expanded (Fig. 3E,F,O,P). Expression of *Tbx6* and *Msgn1* was expanded by 5099 (Fig. 3I,J,Q,R), an effect that was more pronounced at higher doses (supplementary material Fig. S10I,J,Q,R). Somitomere markers *Thyl2* and *Ripply2* showed thicker domains; S–III expanded to the posteriormost edge of the embryo where somites are not found in controls (Fig. 3G,H). At non-receptor-selective doses, 4647 exacerbated the phenotypes of *Msgn1*, *Tbx6* and *Ripply2* (supplementary material Fig. S10E,F,H,O,P) and promoted ectopic expression of *Thyl2* in the midline, with somitomeres occupying nearly the entire anteroposterior axis (supplementary material Fig. S10G). By contrast, 5099 treatment produced fewer, thinner somitomeres (Fig. 3K,L), an effect more pronounced at higher doses (supplementary material Fig. S10K,L).

Since *Rarγ2* is co-expressed with *Msgn1*, we expected that 4647 would reduce and 5099 would expand *Rarγ2* expression. *Rarγ2* expression was expanded by inverse agonist and reduced by agonist (Fig. 2F) as verified by QPCR (supplementary material Fig. S11), which is surprising given that other receptor subtypes (RARα2 and RARβ2) are induced by agonist (Leroy et al., 1991; Sucov et al., 1990). The data indicate that 5099 enhances repression by RARγ, increasing caudal gene expression, whereas 4647 relieves repression by RARγ, diminishing caudal gene expression.

Relief of repression reduces domains of posterior Hox and PSM markers

Treatment with 4647 activates RARγ and removes repressors from RARγ targets, creating posterior truncations. We hypothesized that loss of RARγ2 would phenocopy 4647 treatment once RARγ2-mediated repression was lost. We designed AUG MOs to capture both pseudoalleles of *Rarγ2*. Knockdown of RARγ2.1/2.2 resulted in loss of *Hoxc10*, *Hoxd10*, *Hoxa11* and *Hoxc13* expression, together with severe curvature and reduction of the injected side (Fig. 4A-D). Microinjection of splice-blocking MO capturing both pseudoalleles of *Rarγ2* reduced the expression of *Rarγ2* as measured by QPCR, phenocopying the AUG MOs (supplementary material Fig. S12). We demonstrated that axial truncation on the injected side was not due to developmental delay (supplementary material Fig. S13). To establish that RARγ2 is solely responsible for the axial truncations and reduction in posterior Hox and PSM domains, we showed that *Rarγ2* MO can only be rescued with *Rarγ2*, but not *Rarα2* or *Rarβ2*, mRNA (Fig. 5). RARγ2 knockdown reduced and shifted the expression of *Msgn1* and *Tbx6* anteriorly along the midline (Fig. 4E,F,I-J′) and caused an anterior shift in the paraxial domains of *Thyl2* and *Ripply2*, while obliterating lateral expression (Fig. 4G,H). The complexity of the *Rarγ2* MO phenotype is likely to be due to the fact that RARγ2 knockdown both disrupts its repressive function in the absence of ligand and its activation in the presence of ligand, particularly near the determination wavefront.

When the dominant-negative co-repressor c-SMRT is overexpressed, it binds RAR and blocks recruitment of co-repressors (Chen et al., 1996). We identified several c-SMRT isoforms from *Xenopus*, selecting that most similar to human c-SMRT that we used previously. Microinjection of *Xenopus laevis* (Xl) *c-smrt* mRNA relieved

Development (2014) 141, 2260-2270 doi:10.1242/dev.103705

repression by GAL4-xRARγ in whole embryos (supplementary material Fig. S14). This effect was potentiated by addition of 1 μM TTNPB (supplementary material Fig. S14). Overexpression of Xl *c-smrt* mRNA caused significant reductions in the neural and lateral domains of *Hoxc10* and *Hoxd10* (Fig. 6B,D). Xl *c-smrt* also reduced *Hoxc13*, *Tbx6*, *Msgn1* and *xNot* (Fig. 6F,H,H′,J,J′,L). Similar to *Rarγ2* MO, moderate truncation of injected axes was observed in 70% of embryos, but the midline, rostral shifting of *Tbx6* and *Msgn1* (as in *Rarγ2* MO embryos) was minimal. We conclude that Xl c-SMRT relieves repression of *Rarγ2*, causing loss of progenitor and PSM cells and posterior Hox gene expression.

Another method for relieving repression is overexpression of constitutively active VP16-RARγ2 (RARγ2 fused to the VP16 activation domain). Microinjection of VP16-*Rarγ2* mRNA led to a truncated axis on the injected side in 100% of embryos and loss of *Hoxc10*, *Hoxd10*, *Msgn1* and *Tbx6* expression (Fig. 7). These embryos were less curved than *Rarγ2* MO-injected or *c-smrt*-injected embryos, but rostral expansion of neural/midline and lateral domains was consistently observed, similar to *Rarγ2* MO embryos.

Increased repression expands posterior Hox and PSM markers

Treatment with 4647 or microinjection of *c-smrt* or VP16-*Rarγ2* mRNA relieved repression by RARγ, increasing RAR signaling, decreasing posterior Hox and PSM markers. Decreasing RAR signaling should produce the opposite effect. We microinjected mRNA overexpressing the RA catabolic enzyme CYP26A1 and observed rostral shifts in the lateral and neural expression domains of *Hoxc10* and *Hoxd10* (supplementary material Fig. S15). Microinjection of dominant-negative (DN)-RARγ2 should phenocopy 5099 treatment because co-repressors would be retained on RARγ2 targets, leading to repression. Overexpression of DN-RARγ2 increased the expression of *Msgn1* and *Tbx6* in both lateral and paraxial domains, and shifted *xNot* expression rostrally

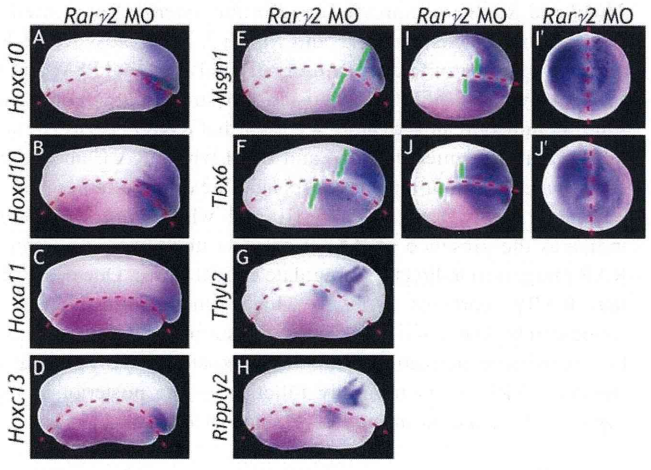

Fig. 4. RARγ2 knockdown alters expression of posterior Hox and PSM markers. (A-J′) Embryos were injected unilaterally at the 2- or 4-cell stage with 7.5 ng *Rarγ2.1* MO+7.5 ng *Rarγ2.2* MO. Injected side is indicated by magenta β-gal lineage tracer. *Rarγ2.1/2.2* MO decreases expression of (A) *Hoxc10* (18/18 embryos), (B) *Hoxd10* (12/12), (C) *Hoxa11* (9/9) and (D) *Hoxc13* (16/16) in tailbud stage embryos. *Rarγ2.1/2.2* MO decreases lateral, but expands midline, expression (green lines) of (E) *Msgn1* (10/13) and (F) *Tbx6* (8/11), knocking down and shifting expression rostrally of (G) *Thyl2* (13/15) and (H) *Ripply2* (13/14) in tailbud stage embryos. *Rarγ2.1/2.2* MO decreases lateral, but expands midline, expression (green lines) of (I) *Msgn1* (35/36) and (J) *Tbx6* (20/20) in neurula stage embryos. Embryos shown in dorsal view with anterior on left. (I′,J′) Caudal views of I and J.

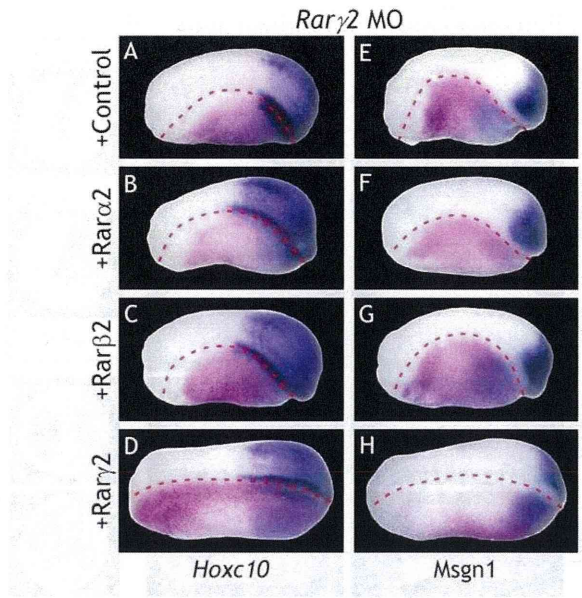

Fig. 5. *Rarγ2* mRNA rescues posterior Hox and PSM expression in *Rarγ2* MO embryos. (A-H) Embryos injected unilaterally at 2- or 4-cell stage. Injected side is indicated by magenta β-gal lineage tracer. (A,E) 5 ng *Rarγ2.1* MO+5 ng *Rarγ2.2* MO+control (*mCherry*) mRNA diminishes *Hoxc10* and *Msgn1* expression, curving the embryo axis in 100% of embryos (*Hoxc10*, 23/23; *Msgn1*, 13/13). (B,C,F,G) Co-injection of *Rarγ2* MO and 1 ng *Rarα2* mRNA or 1 ng *Rarβ2* does not rescue the phenotype; however, (D,H) 1 ng *Rarγ2* mRNA partially rescues axial curvature and *Hoxc10* (18/23) and *Msgn1* (23/35) expression. Tailbud embryos shown in dorsal view with anterior to left.

(Fig. 8B,D,F). DN-RARγ2 phenocopied the effects of *Cyp26a1* mRNA (Moreno and Kintner, 2004) on somitomere markers *Thyl2* and *Ripply2;* rostral shifting and knockdown of somitomere expression was the phenotype that we observed (Fig. 8H,J,K).

Microinjection of *Rarγ2* MO alone resulted in knockdown of *Hoxc10* and axial truncation (Fig. 9A,B,E). We hypothesized that this phenotype was due to loss of repression, reasoning that the phenotype should be rescued with DN-RARγ2. Axial defects and lateral knockdown of *Hoxc10* expression were partially recovered with DN-*Rarγ2* mRNA (Fig. 9C,D,E). The neural domain of *Hoxc10* expression was rescued in nearly all embryos and a rostral shift often observed. We conclude that increasing repression with DN-RARγ2 or overexpressing CYP26A1 (removing ligand) promotes caudal gene expression, similar to chemical treatment with 5099. Moreover, loss of caudal structures and gene expression due to *Rarγ2* MO are rescued by restoring repression with DN-RARγ2.

DISCUSSION

RARγ repression in caudal development

Most studies consider only one aspect of RAR signaling, namely its role as a ligand-activated transcription factor promoting the expression of target genes. In developmental biology, RA signaling has been studied extensively for its ability to promote differentiation and establish boundaries in somitogenesis, neurogenesis and rhombomere segmentation (reviewed by Rhinn and Dolle, 2012). Liganded RAR has been predicted to function passively in the caudal region until required to facilitate body axis cessation (Olivera-Martinez et al., 2012), when somitogenesis is nearing completion because the determination wavefront, moving the RA source caudally, has exhausted the progenitor cell pool (Gomez and Pourquie, 2009). Here, liganded RARγ would function as an activator promoting apoptosis (Shum et al., 1999) at terminal tailbud stage. However, this does not address why RARγ2 would be highly expressed where RA is